

# The Diffuse Supernova Neutrino Background

JOHN F. BEACOM

*Department of Physics,  
Department of Astronomy,  
and Center for Cosmology and Astro-Particle Physics,  
The Ohio State University,  
191 West Woodruff Avenue, Columbus, Ohio 43210, USA*  
*beacom.7@osu.edu*

**Key Words** neutrino astronomy, massive stars, cosmic backgrounds

**Abstract** The Diffuse Supernova Neutrino Background (DSNB) is the weak glow of MeV neutrinos and antineutrinos from distant core-collapse supernovae. The DSNB has not been detected yet, but the Super-Kamiokande (SK) 2003 upper limit on the  $\bar{\nu}_e$  flux is close to predictions, now quite precise, based on astrophysical data. If SK is modified with dissolved gadolinium to reduce detector backgrounds and increase the energy range for analysis, then it should detect the DSNB at a rate of a few events per year, providing a new probe of supernova neutrino emission and the cosmic core-collapse rate. If the DSNB is not detected, then new physics will be required. Neutrino astronomy, while uniquely powerful, has proven extremely difficult – only the Sun and the nearby Supernova 1987A have been detected to date – so the promise of detecting new sources soon is exciting indeed.

## CONTENTS

Introduction . . . . .	3
Impossible Dreams of Neutrino Astronomy . . . . .	4
Framework: DSNB Detection Spectrum at Earth . . . . .	4
<i>Simple Estimate of the Detection Rate</i> . . . . .	5
<i>Line of Sight Integral for the DSNB Flux</i> . . . . .	5
<i>Contemporary Inputs, Uncertainties, and Detectors</i> . . . . .	6
<i>Theoretical Predictions and Experimental Revolutions</i> . . . . .	7
First Ingredient: Supernova Neutrino Emission . . . . .	8
<i>The Fates of Massive Stars</i> . . . . .	8
<i>Core-Collapse Supernova Neutrino Emission</i> . . . . .	9
<i>Comparison to Supernova 1987A</i> . . . . .	10
Second Ingredient: Cosmic Supernova Rate . . . . .	11
<i>Measured Star Formation Rate</i> . . . . .	11
<i>Predicted Supernova Rate</i> . . . . .	12
<i>Measured Supernova Rate</i> . . . . .	12
Third Ingredient: Neutrino Interactions and Detectors . . . . .	14
<i>Detection of DSNB Electron Antineutrinos</i> . . . . .	14
<i>The Super-Kamiokande Detector</i> . . . . .	15
Framework Redux: DSNB Detection Spectrum at Earth . . . . .	15
Super-Kamiokande 2003 Upper Limit on the DSNB . . . . .	15
<i>Detector Backgrounds and DSNB Flux Limit</i> . . . . .	16
<i>Calculated Limits on Supernova Neutrino Emission</i> . . . . .	17
Pathways to Discovery . . . . .	18
<i>Proposal for Background Reduction in SK</i> . . . . .	18
<i>Research and Development for Gadolinium in SK</i> . . . . .	20
<i>Prospects for Other Detectors and Flavors</i> . . . . .	20
Conclusions . . . . .	20

## 1 Introduction

The Diffuse Supernova Neutrino Background (DSNB) is the flux of neutrinos and antineutrinos emitted by all core-collapse supernovae in the causally-reachable universe; it will appear isotropic and time-independent in feasible observations. (Hereafter, neutrinos means neutrinos and antineutrinos, and supernovae means core-collapse supernovae, unless specified.) It results from the quasi-thermal MeV neutrino spectrum emitted by newly-formed neutron stars convolved with the rapid redshift evolution of the supernova rate. The cosmic energy density in neutrinos from core-collapse supernovae is comparable to that in photons from stars,  $\sim 0.01 \text{ eV cm}^{-3}$ , and is  $\sim 10$  times less than that of the cosmic microwave background. Some earlier literature referred to “supernova relic neutrinos,” but “relic” often caused confusion with the  $10^{-4} \text{ eV}$  neutrinos from the Big Bang.

Why is detection of the DSNB an important and relevant experimental goal?

- **Understanding supernovae is crucial to astrophysics and physics.** Supernovae are central to the cosmic history of stellar birth and death; the production of chemical elements, neutron stars and black holes, cosmic rays, and gravitational waves; and to exploiting the extreme physical conditions of core collapse to probe the properties of neutrinos and hypothetical particles. New observations and syntheses are needed.

- **We cannot understand supernovae without detecting neutrinos.** The optical supernova reveals little about the collapsing core itself, which is embedded in the stellar envelope; the total energy in photons is much less than that in neutrinos, leaves over a vastly longer time, and depends on the properties of the progenitor star. Neutrinos are emitted from the core, revealing its properties.

- **Detecting bursts of neutrinos from nearby supernovae is difficult.** Prodigious emission and large detectors partially compensate the tiny detection cross section. For Milky Way supernovae (distance  $D \sim 10 \text{ kpc}$ ;  $1 \text{ pc} = 3.1 \times 10^{18} \text{ cm}$ ), a neutrino burst would be detected easily, but the burst rate is only a few per century. For supernovae in nearby galaxies ( $D \sim 1\text{--}10 \text{ Mpc}$ ), where the total burst rate is above one per year, much larger detectors will be required.

- **The DSNB is a guaranteed steady source of supernova neutrinos.** While the probability of detecting even a single neutrino from a distant supernova is infinitesimally small, the number of supernovae per year is astronomically large, yielding a nonzero rate. The total rate and spectral shape of the DSNB are new probes of supernova neutrino emission and the cosmic core-collapse rate.

*The DSNB has not been detected yet, but the discovery prospects are excellent.* Super-Kamiokande (SK) is large enough to detect the DSNB at the level of a few events per year. These events are hidden by detector backgrounds, which are already low and could be substantially reduced with added gadolinium to detect neutrons, a proposed upgrade for which there is active research and development.

Detection of the DSNB will yield science that is difficult to obtain otherwise. It will measure the average supernova neutrino emission spectrum, and comparison to burst detections will probe the star-to-star variation. It will also be sensitive to the optically-dark failed supernovae expected from high-mass stars.

This review is written for experimentalists, observers, and theorists in nuclear physics, particle physics, and astrophysics, and covers the many aspects of the DSNB. It is intended to be an accessible overview of the main themes needed to predict, detect, and interpret the DSNB, with details given in references.

## 2 Impossible Dreams of Neutrino Astronomy

Neutrino astronomy is a unique tool for answering some of the oldest and most important questions in nuclear and particle astrophysics (1). What happens when a massive star runs out of fuel? Are observed high-energy gamma ray sources powered by cosmic-ray protons or electrons? What is the origin of the highest-energy cosmic rays? Are there astrophysical neutrino sources unseen with electromagnetic observations? Are there new properties of neutrinos, or new particles, that can be revealed only with neutrino detectors?

The immense discovery potential of neutrino astronomy arises from the small interaction cross section of neutrinos with matter, which allows neutrinos to escape from and thus to reveal the interiors of dense and distant astrophysical objects, undeflected, undegraded, and unobscured. This powerful magic comes at a terrible price, as it is much less likely that the neutrinos will interact with a detector than with an entire star. As far as we know, neutrinos interact only via the weak nuclear force and gravity (but with only tiny masses).

In 1934, shortly after Pauli postulated the existence of the neutrino, Bethe and Peierls wrote that “If [there are no new forces] – one can conclude that there is no practically possible way of observing the neutrino” (2). It took until 1956 for neutrinos to be detected, by Reines and Cowan, using a nuclear reactor source (3), for which Reines shared in the 1995 Nobel Prize (Cowan died in 1974). This detection allowed a first consideration of neutrino astronomy in principle.

Prescient remarks about this potential were made long ago, e.g., Refs. (4–8). As Bahcall wrote in 1964 about solar neutrinos, before their detection, “Only neutrinos, with their extremely small interaction cross sections, can enable us to see into the interior of a star...” (9). The detection of neutrinos from the Sun and the nearby Supernova 1987A (SN 1987A) shows that the required sensitivity has begun to be reached. Davis and Koshiba shared in the 2002 Nobel Prize for these first detections in neutrino astronomy, which led a precise understanding of the solar fusion reactions, the discovery of neutrino mixing, and confirmation that Type II supernovae result from the deaths of massive stars.

No other astrophysical neutrinos have been detected, despite decades of effort. In Bahcall’s 1989 book, *Neutrino Astrophysics*, which was almost completely about solar neutrinos, he wrote that “The title is more of an expression of hope than a description of the book’s contents...the observational horizon of neutrino astrophysics may grow ... perhaps in a time as short as one or two decades” (10). Indeed, the first detections of distant neutrino sources now seem imminent, due to more certain predictions, based on new astronomical and laboratory data, and due to astounding improvements in detector sensitivity. Any detections will be of enormous scientific importance, certain to provide new information.

This review is about the exciting prospects for new results in extrasolar MeV neutrino astronomy; as described below, these build on a long history of work in experiment, observation, and theory. There are similarly encouraging prospects at the TeV ( $10^6$  MeV) scale (11,12) and the EeV ( $10^{12}$  MeV) scale (12,13).

## 3 Framework: DSNB Detection Spectrum at Earth

Here the framework to calculate the DSNB detection spectrum is given, along with a summary of its three ingredients: the supernova neutrino emission (Section 4), the cosmic supernova rate (Section 5), and the detector capabilities (Section

6), followed by a return to the framework (Section 7), then SK observations (Section 8), background reduction (Section 9), and conclusions (Section 10).

### 3.1 Simple Estimate of the Detection Rate

SN 1987A was discovered optically in the Large Magellanic Cloud, a nearby satellite of the Milky Way, at a distance of about 50 kpc (14). Since it was so close, it was likely that its neutrinos had interacted in the Kamiokande-II (Kam-II) and Irvine-Michigan-Brookhaven (IMB) water-Čerenkov detectors, originally intended for proton decay searches. Kam-II reported 12 events and IMB reported 8 events, with energies of several tens of MeV, in contemporaneous bursts of about 10 seconds, occurring a few hours before the optical brightening (15–18). The events were largely consistent with being due to inverse beta decay,  $\bar{\nu}_e + p \rightarrow e^+ + n$ , where the positron is detected, and where its energy is close to that of the neutrino.

Deferring many details, we can simply estimate the (steady) detection rate of DSNB neutrinos from the (burst) detection rate of SN 1987A neutrinos, as

$$\left[ \frac{dN_\nu}{dt} \right]_{DSNB} \sim \left[ \frac{dN_\nu}{dt} \right]_{87A} \left[ \frac{N_{SN} M_{det}}{4\pi D^2} \right]_{87A}^{-1} \left[ \frac{N_{SN} M_{det}}{4\pi D^2} \right]_{DSNB}. \quad (1)$$

The detection rate in Kam-II during the burst was  $\sim 1 \text{ s}^{-1}$ . How are the inputs for the dimensionless product of conversion factors related? For SN 1987A,  $N_{SN} = 1$ , while there are  $N_{SN} \sim 100$  neutrino bursts in the universe starting within any 10-second interval; this accounts for the supernova rate of the Milky Way,  $\sim 10^{-2} \text{ year}^{-1}$ , the space density of comparable galaxies,  $\sim 10^{-2} \text{ Mpc}^{-3}$ , and the fact that the supernova rate per galaxy was  $\sim 10$  times higher in the past. The detector mass  $M_{det}$  of Kam-II was  $\sim 10$  times smaller than that of SK, which is 22.5 kton ( $22.5 \times 10^9 \text{ g}$ ). The distance  $D$  of SN 1987A was 0.050 Mpc, whereas for a typical supernova contributing the DSNB, at  $z \sim 1$ , it is  $c/H_0 \sim 4000 \text{ Mpc}$ ,  $\sim 10^5$  times farther. Then the time-averaged DSNB detection rate in SK, noting changes in  $N_{SN}$ ,  $M_{det}$ , and  $1/D^2$ , respectively, is

$$\left[ \frac{dN_\nu}{dt} \right]_{DSNB} \sim (1 \text{ s}^{-1}) \times 100 \times 10 \times 10^{-10} \sim 10^{-7} \text{ s}^{-1} \sim 3 \text{ year}^{-1}, \quad (2)$$

which is about the right number.

The Poisson expectation for the number of neutrinos detected per supernova is  $\ll 1$ , so nearly all supernovae will yield 0, and a rare few unidentified supernovae will yield just 1. While the long-term average of the neutrino detection rate from Milky Way supernovae is  $\sim 100$  times larger than for the DSNB, it requires waiting decades for large bursts from single identified supernovae. Future very large detectors may detect more frequent, but much smaller, bursts from identified supernovae in the nearest galaxies. Burst detection will be required to study the time profile and flavor dependence of supernova neutrino emission.

### 3.2 Line of Sight Integral for the DSNB Flux

The DSNB flux spectrum at Earth is calculated from the neutrino emission per supernova  $\varphi(E_\nu)$  and the evolving core-collapse supernova rate  $R_{SN}(z)$  as

$$\frac{d\phi}{dE_\nu}(E_\nu) = \int_0^\infty [(1+z) \varphi(E_\nu(1+z))] [R_{SN}(z)] \left[ \left| \frac{c dt}{dz} \right| dz \right], \quad (3)$$

where this form arises as a standard line-of-sight integral for the radiation intensity (flux per solid angle) from a distribution of sources. Neglecting cosmological factors, the differential injection rate of neutrinos depends on the rate density (the number of neutrinos emitted per volume and time, i.e., the supernova neutrino emission times the supernova rate density) times the volume element  $d\Omega r^2 dr$ , while the fluxes fall off as  $1/(4\pi r^2)$ , canceling the  $r^2$ . The received intensity is then just a line integral of the rate density. Since the sources are isotropic on the sky, the detection reaction has little directionality, and Earth is transparent to neutrinos, the intensity has been integrated over  $4\pi$  to obtain the flux.

This defines the neutrino number flux spectrum, in units  $\text{cm}^{-2} \text{s}^{-1} \text{MeV}^{-1}$ . To obtain the energy flux spectrum, more familiar to photon astronomers, multiply through by  $E_\nu$ . The first term in large brackets is the emission spectrum  $\varphi(E_\nu)$ , where a neutrino received at energy  $E_\nu$  was emitted at a higher energy  $E_\nu(1+z)$ ; the prefactor of  $(1+z)$  on the spectrum accounts for the compression of the energy scale. The second term is the supernova rate density  $R_{SN}(z)$ . The third term is the differential distance, where  $|dt/dz|^{-1} = H_0(1+z)[\Omega_\Lambda + \Omega_m(1+z)^3]^{1/2}$ , the cosmological parameters are  $H_0 = 70 \text{ km s}^{-1} \text{Mpc}^{-1}$ ,  $\Omega_m = 0.3$ ,  $\Omega_\Lambda = 0.7$ , and their uncertainties can be neglected.

Above, it is assumed that there is no variation in the supernova neutrino emission among different progenitor stars, which follows from the core-collapse criterion for massive stars and how supernova neutrino mixing effects work, both discussed in Section 4.2. It is also assumed that nothing except redshifting happens to the neutrinos between the supernovae and Earth, as obscuration is always negligible, the neutrino mass eigenstates that propagate do not oscillate, and no exotic effects are expected (but such can be tested (19–22)). These are realistic assumptions at the precision of the expected counts and energy resolution, and can be generalized with appropriate averages.

### 3.3 Contemporary Inputs, Uncertainties, and Detectors

Throughout, we focus on the effective  $\bar{\nu}_e$  spectrum at the surface of the supernovae, after any neutrino mixing effects in the star, as this is the same observable for both burst and DSNB detection. As described in Section 4, the neutrino emission in one flavor is characterized by its total energy (time-integrated luminosity) and average energy ( $3.15T$  for a Fermi-Dirac spectrum, where  $T$  is the temperature in units of MeV). These are the parameters to be determined by a DSNB measurement, as the supernova neutrino emission is now the most uncertain input, and it cannot be measured by astronomical techniques. Nominal values are  $E_{\bar{\nu}_e, \text{tot}} \sim 5 \times 10^{52} \text{ erg}$  ( $3 \times 10^{58} \text{ MeV}$ ), and  $E_{\bar{\nu}_e, \text{avg}} \sim 15 \text{ MeV}$ . If a black hole forms promptly, the luminosity from the collapsing core prior to being abruptly terminated can be higher than for neutron star formation, yielding a larger time-integrated emission (24).

The cosmic supernova rate is now well measured, as shown in Section 5. For the supernova rate density, the local value is  $\simeq (1.25 \pm 0.25) \times 10^{-4} \text{ Mpc}^{-3} \text{ year}^{-1}$ , and the rate grows by a factor  $\simeq 10$  by  $z = 1$ . DSNB measurements are also sensitive to core collapses that are optically dark but neutrino bright.

**Figure 1** shows the  $\bar{\nu}_e$  flux spectrum; the SK 2003 limit is  $\lesssim 1.2 \text{ cm}^{-2} \text{ s}^{-1}$  for energies integrated above 19.3 MeV, ruling out spectra above about the middle of the  $T = 8 \text{ MeV}$  band. Since the predictions are for generic thermal spectra, they could be used for other flavors as well. Equation (3) defines the *flux spectrum* of

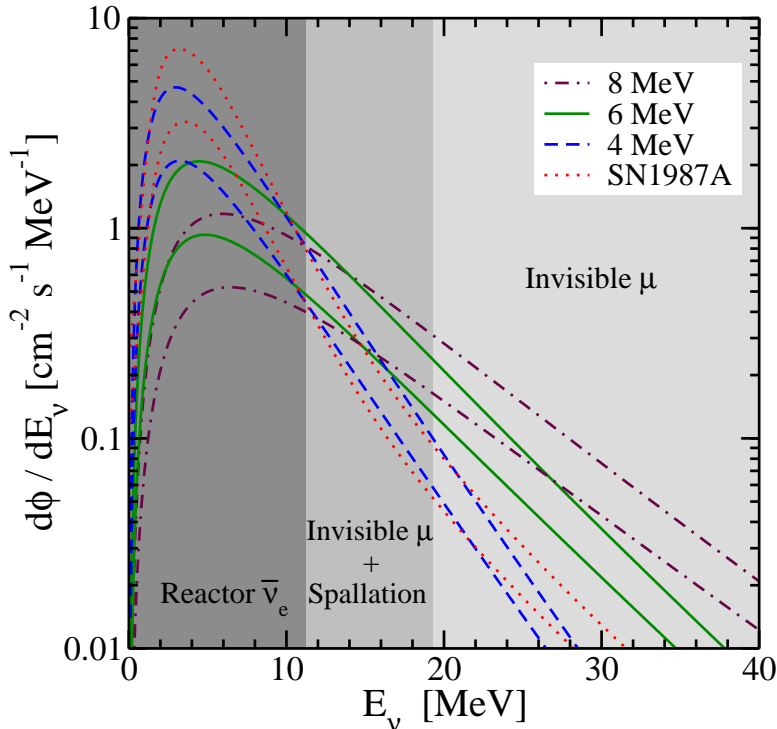


Figure 1: **Predicted DSNB  $\bar{\nu}_e$  flux spectrum.** The spread between different labeled temperature bands indicates the uncertainty in the supernova neutrino emission; the widths of the bands indicates the uncertainty in the cosmic supernova rate. Grey shaded regions indicate energy ranges where noted detector backgrounds are important. Figure as shown in Ref. (23).

neutrinos. In Section 6, the *event rate spectrum* of positrons from the reaction  $\bar{\nu}_e + p \rightarrow e^+ + n$  is introduced to allow comparison with the SK data.

### 3.4 Theoretical Predictions and Experimental Revolutions

Theoretical predictions of the DSNB flux go back more than forty years, e.g., to brief mentions by Zel'dovich and Guseinov (25) and Ruderman (8), and a calculation by Guseinov (26). First examples of detailed calculations, from the early 1980s, are Refs. (27–34); unfortunately, the true flux is not as large as in these predictions (but see the pessimistic lower limit noted in Ref. (33)). The variation between predictions, formerly orders of magnitude, became much less beginning in the mid-1990s, in e.g., Refs. (35–45). At roughly the end of that era, the DSNB was reviewed in 2004 by Ando and Sato (46). The SK 2003 upper limit on the DSNB was a key development, as it directly rules out models with fluxes more than a few times larger than present predictions.

It would be unfair to judge earlier predictions without adjusting their inputs to contemporary values. This seems difficult, as a wide variety of different formalisms, inputs, standards of precision, and methods of quoting results were used. However, this is easy in the present perspective, first noted in Ref. (47), where the principal remaining unknown is the supernova neutrino emission, and the assumed values could be easily extracted from earlier papers. In fact, most

DSNB predictions did use reasonable supernova neutrino emission parameters (for the earliest papers, the existence of  $\nu_\tau$  and  $\bar{\nu}_\tau$  was unknown), even before the detection of SN 1987A. There were huge differences in the supernova rate density assumed, due to uncertainties that have been dramatically reduced by comprehensive star formation and supernova rate measurements over the past decade. The results shown in this review cover the range of reasonable allowed models for both the supernova neutrino emission and the supernova rate density.

## 4 First Ingredient: Supernova Neutrino Emission

The detection of neutrinos from SN 1987A established that *some* supernovae produce *some* neutrinos. Of course, our knowledge is much greater than that – there is strong evidence that core-collapse supernovae can be identified optically, and that a powerful neutrino burst must accompany core collapse.

To understand the properties of massive stars and how supernovae explode, it is necessary to confirm the ubiquity of neutrino emission from all types of supposed core-collapse supernovae and to refine our knowledge of this emission.

### 4.1 The Fates of Massive Stars

Massive stars race towards their doom. The lifetime of a star, mostly the time spent burning hydrogen in the core, is  $\sim 30 (8M_\odot/M)^{2.5} \times 10^6$  year, where  $M_\odot = 2.0 \times 10^{33}$  g is the solar mass (48). The fusion reactions proceed in stages that depend on temperature, overcoming the Coulomb barriers for successively heavier elements only once the preceding elements are exhausted and the core contracts. Only stars with mass greater than about  $8M_\odot$  will become hot and dense enough in the core to burn past carbon and oxygen to iron (49, 50). A Chandrasekhar instability sets in once about  $1.4M_\odot$  of iron has been created, since no further nuclear reactions can generate energy and electron degeneracy pressure provides insufficient support. Photo-nuclear reactions then endothermically destroy iron, leading to further collapse, which continues until the core reaches nuclear densities and cannot be compressed further. The subsequent bounce leads to the formation of an outgoing shock, which removes the envelope of the star and causes the optical supernova, which is bright for several months. What will be left behind is a neutron star or black hole from the core and a shell remnant from the envelope.

Astronomical characterizations of supernovae are based on their optical properties (51). Supernovae must be distinguished by their spectra, as their light curves alone are not usually enough. Many lines of evidence indicate that Types II, Ib, and Ic supernovae arise from the core collapse of massive stars, differing in the amount of progenitor envelope mass loss before explosion. Type II supernovae are several times more common than Types Ib and Ic, and the latter two seem to arise from ranges of successively larger progenitor mass. All should have comparable emission of all flavors of neutrinos and antineutrinos, due to the mechanism of core collapse. Type Ia supernovae, which are also several times less common than Type II supernovae, seem to be powered by the runaway thermonuclear burning of a carbon and oxygen white dwarf in a binary system into iron; only relatively modest emission of low-energy electron neutrinos is expected. Detecting neutrinos will test the mapping between optical supernova types and underlying physical mechanisms (52).



## 4.2 Core-Collapse Supernova Neutrino Emission

The basic picture of core collapse is well known (53). When the core collapses, there is a huge change in its gravitational potential energy. For a constant density profile, the change in this self-energy is

$$\Delta(P.E.) \simeq \left( \frac{3G_N M^2}{5R} \right)_{NS} - \left( \frac{3G_N M^2}{5R} \right)_{core} \simeq 3 \times 10^{53} \text{ erg}, \quad (4)$$

where the number follows from the mass and radius of a typical neutron star,  $1.4 M_\odot$  and 10 km (the subtracted term is negligible since the initial core radius is thousands of kilometers), and this is an incredible  $\sim 10\%$  of  $Mc^2$  for the core (54–56). The mass of the collapsed core varies little with the mass of the progenitor star (57, 58). Since the proto-neutron star is near nuclear density, no particles except neutrinos can escape, and core collapse is inevitably accompanied by a huge burst of neutrinos, carrying away nearly the whole change in gravitational potential energy. The neutrinos, which begin leaving the core at the instant of collapse, arrive at Earth before the light, which is delayed by at least the time it takes the shock to propagate through the envelope, typically hours. This was observed for SN 1987A, and is a crucial confirmation of the basic picture.

It is thought that each of the six flavors of neutrinos and antineutrinos carries away a comparable fraction of the total energy. In numerical simulations of supernovae, this equipartition is only approximate, and the sense in which it might be violated in nature is not known (59–62). Most of the neutrino emission is in pairs,  $\bar{\nu}_e + \nu_e$ ,  $\bar{\nu}_\mu + \nu_\mu$ , and  $\bar{\nu}_\tau + \nu_\tau$ , that are produced by weak interactions in the hot and dense matter in the core. The reaction  $e^- + p \rightarrow \nu_e + n$  converts the nearly equal numbers of neutrons and protons from nuclei into the neutron-rich matter of the neutron star, producing an excess  $\nu_e$  flux, but this is a  $\sim 10\%$  effect.

The proto-neutron star density is so high that even neutrinos do not readily escape, and instead diffuse out over several seconds, and are thus emitted with a quasi-thermal spectrum characteristic of the surface of last scattering. If the proto-neutron star were semi-transparent, the neutrinos would leave on a timescale of  $\sim 1$  millisecond, with energies of  $\sim 100$  MeV. Taking opacity into account, and assuming blackbody emission,  $L \sim E_{tot}/\tau \sim R^2 T^4$ , the increase in the emission time by  $\sim 10^4$  corresponds to the decrease in neutrino average energy by  $\sim 10$ . A long emission timescale and moderate temperature were observed for SN 1987A, confirming the high density of the proto-neutron star.

The opacities of neutrino flavors with matter vary, leading to different neutrino temperatures, since the matter temperature of the proto-neutron star falls with radius. The interactions of  $\nu_\mu$ ,  $\nu_\tau$ ,  $\bar{\nu}_\mu$ ,  $\bar{\nu}_\tau$  are only through the weak neutral current, since their energies are too low to produce the corresponding charged leptons. For  $\nu_e$  and  $\bar{\nu}_e$ , there are also interactions through the weak charged current, so the cross sections are larger; for  $\nu_e$ , the coupling constants are larger and there are more neutron than proton targets. Oft-quoted estimates for the temperatures are  $T = 8$  MeV for  $\nu_\mu$ ,  $\nu_\tau$ ,  $\bar{\nu}_\mu$ ,  $\bar{\nu}_\tau$ ,  $T = 5$  MeV for  $\bar{\nu}_e$ , and  $T = 4$  MeV for  $\nu_e$ . More recent theoretical work indicates that the temperatures, and the splittings between them, are less (64).

Neutrino mixing effects relate the initial neutrino spectra at the opaque emitting surface of the proto-neutron star to those outside the supernova. While the opacity is low outside the neutron star, the high density of matter and even other neutrinos significantly affects neutrino mixing (65–68). The passage through high

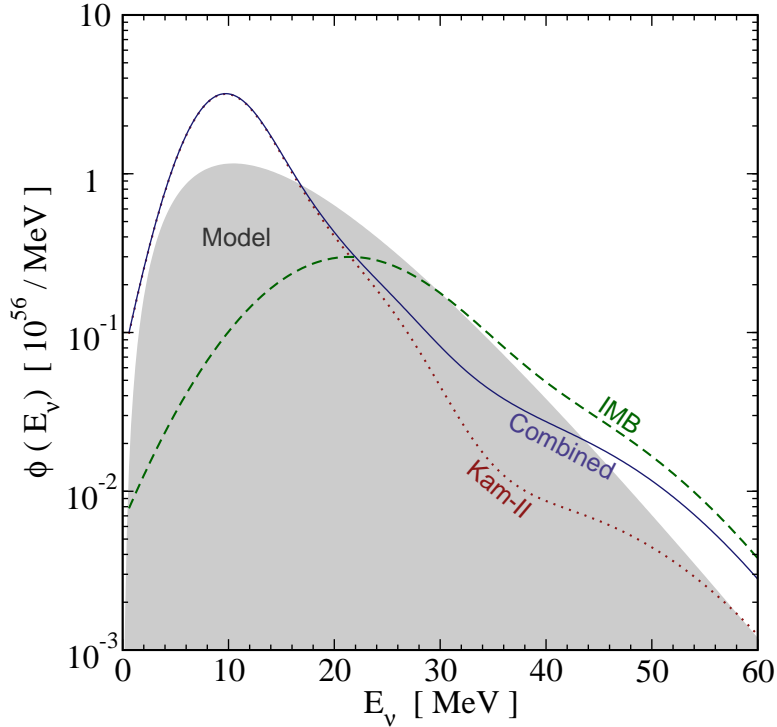


Figure 2: **Time-integrated effective  $\bar{\nu}_e$  spectrum from SN 1987A.** The curves indicate results reconstructed using only the Kam-II data, the IMB data, or their combination. The grey shaded region is a thermal spectrum with parameters  $E_{\bar{\nu}_e, tot} \sim 5 \times 10^{52}$  erg and  $E_{\bar{\nu}_e, avg} \sim 15$  MeV. Figure as shown in Ref. (63).

densities leaves the neutrinos in incoherent mass eigenstates that do not oscillate between the supernova and Earth. Mixing effects in Earth are suppressed by the isotropy of the sources and the detection cross section (69).

Neither the expected initial spectra nor the neutrino mixing effects are understood well enough, so we use the observable effective spectra. For  $\bar{\nu}_e$ , the effective time-integrated spectrum after mixing, assumed to approximately be of the Fermi-Dirac form, in units  $\text{MeV}^{-1}$ , is

$$\varphi(E_\nu) = E_{\bar{\nu}_e, tot} \frac{120}{7\pi^4} \frac{E_\nu^2}{T^4} \frac{1}{(e^{E_\nu/T} + 1)}, \quad (5)$$

where the total energy is  $E_{\bar{\nu}_e, tot}$  and the average energy is  $E_{\bar{\nu}_e, avg} = 3.15 T$ . These parameters are not fixed from theory, but will be determined from experiment, and will test supernova simulations and neutrino mixing scenarios.

### 4.3 Comparison to Supernova 1987A

While the SN 1987A data were sparse, and the detectors were not optimized for that purpose, these data are the most direct evidence we have about supernova neutrino emission. A reconstruction of the effective  $\bar{\nu}_e$  spectrum from the Kam-II and IMB data is shown in **Figure 2**; it is in reasonable agreement with expectations. Higher temperatures are favored by theoretical models including neutrino mixing, as well as by observations of nucleosynthesis yields that depend on high-

energy neutrinos (70–72). It remains to be seen if SN 1987A was different from an average supernova, and more data are needed, especially at high energies.

The SN 1987A data are an important input for estimating the DSNB spectrum (40,45), though care must be taken to note that the high-energy SN 1987A neutrinos are the most relevant for predicting the DSNB (63). The SK 2003 search used a positron energy threshold of 18 MeV, and future searches may reach 10 MeV; redshift effects enhance the importance of high-energy emission.

## 5 Second Ingredient: Cosmic Supernova Rate

Supernovae are infrequent in the Milky Way, but not in the universe. Since massive stars have lifetimes that are very short on cosmological timescales, their cosmic birth and death rates are exactly equal. The cosmic star formation rate has been measured precisely, using a great variety of techniques, principally based on the emission of massive stars. This is enough to accurately give the rate of core collapses, and it is supplemented by direct measurements of the optical supernova rate, which have lower precision, but are in good agreement.

### 5.1 Measured Star Formation Rate

Star formation rate measurements do not literally probe star *formation*, but begin with the total luminosity of the stars in a galaxy. If these stars were all of the same known mass, so that their luminosity and lifetime were given by stellar evolution theory, then the star formation rate would be determined by the total mass of these stars divided by their lifetime; this is the birth (and death) rate needed to keep the number of stars in equilibrium. The main star-formation rate indicators measure the emission from massive stars that are short-lived on galactic timescales, so the equilibrium assumption should be good on average.

A wide range of stellar masses are always present, complicating this procedure, but the degeneracies can be broken, since stars of increasing mass have higher temperatures and much higher luminosities. Massive stars can be isolated by measurements of their continuum flux or of nebular emission lines from atomic recombinations in the surrounding gas they ionize. The distribution of stellar masses formed when star formation occurs is assumed to follow a universal initial mass function (IMF), e.g., the conventional Salpeter IMF scales as  $\psi(M) = dn/dM \propto M^{-2.35}$  for stellar masses  $M$  between  $0.1M_{\odot}$  and  $100M_{\odot}$  (73,74); more realistic IMFs modify the low-mass end. With an IMF, calculated stellar and nebular emission spectra, and careful consideration of the effects of obscuration and re-radiation, the star formation rate can be determined from a galaxy luminosity spectrum (75). The high-mass star formation rate is *measured*, but the formation rate of low-mass stars has to be *deduced* assuming an IMF. This introduces a factor-two range in the normalization of the total star formation rate, due to the low-mass IMF uncertainties.

The comoving star formation rate density, in units  $M_{\odot} \text{ Mpc}^{-3} \text{ year}^{-1}$ , is about ten times larger at  $z = 1$  than it is today, at  $z = 0$ . Comoving coordinates are those for which the expansion of the universe has been removed; crudely, this defines the star formation rate per average galaxy. Aside from the normalization uncertainty due to choice of IMF, the precision of the combined data is at the tens-of-percent level for  $z \lesssim 1$  (23,76). From  $z = 1$  to at least  $z \sim 4 - 5$ , the star formation rate is nearly flat, with a precision becoming as poor as a factor

of two, until a more uncertain decline at higher redshifts, e.g., Refs. (77–82).

These results, especially those in the  $z \lesssim 1\text{--}2$  range relevant for the DSNB, are quite robust, since they have been measured by many different groups using different instruments and techniques, and extensive efforts have been made to calibrate the observables and their corrections for dust obscuration and incompleteness. The star formation rate data are also in good agreement with measurements of the extragalactic background light, which, analogous to the DSNB, is an integral measure of stellar emission over redshifts (23). These and other data favor an IMF of somewhat shallower slope than the Salpeter IMF.

## 5.2 Predicted Supernova Rate

To predict the core-collapse supernova rate density,  $R_{SN}(z)$ , in units  $\text{Mpc}^{-3} \text{year}^{-1}$ , from the star formation rate density,  $R_{SF}(z)$ , we use

$$R_{SN}(z) = R_{SF}(z) \frac{\int_8^{50} \psi(M) dM}{\int_{0.1}^{100} M \psi(M) dM} \simeq \frac{R_{SF}(z)}{143 M_\odot}, \quad (6)$$

where the upper integral gives the number of stars that lead to core collapse and the lower integral gives the total mass in stars, and a Salpeter IMF has been used. Importantly, for  $R_{SN}(z)$  the above-mentioned normalization uncertainty due to the choice of IMF goes away, because nearly the same massive stars source the star formation rate measurements and lead to core-collapse supernovae. For an IMF with a shallower slope,  $R_{SF}(z)$  is smaller, but the ratio of integrals is larger, canceling in  $R_{SN}(z)$  to the few-percent level (23).

In the upper integral, the choice of upper limit of integration is unimportant, as long as it is large; then the integral scales as  $(8M_\odot/M_{lower})^{1.35}$  for a Salpeter IMF. Theoretical and indirect empirical work indicates that the minimum mass star that leads to core collapse is about  $8M_\odot$ . This is now supported by direct observations. Using archival imaging from the Hubble Space Telescope and other sources, it has been possible to identify the stellar progenitors of some supernovae in nearby galaxies, e.g., Refs. (83–86). The luminosity of the star determines its mass, and a fit to progenitor data gives a minimum mass to lead to a core-collapse supernova of  $(8.5 \pm 1.5) M_\odot$  (87). In addition, the largest estimate so far of the maximum mass star that ends instead as a white dwarf is  $\sim 7M_\odot$  (88,89).

There is therefore a precise prediction of the cosmic core-collapse rate, based on strong evidence from star formation rate data and direct confirmation of the minimum stellar mass to lead to a core-collapse supernova. This is based on observations of living massive stars, and does not differentiate whether they will die as visible supernovae or optically-dark collapses. Since those outcomes have comparable neutrino emission, this data is enough to precisely predict the DSNB.

## 5.3 Measured Supernova Rate

As noted, the relationship between star formation and supernova rates is *just a simple conversion* with small uncertainties on the result. Since the redshift evolution of the star formation rate is well measured, the evolution of the supernova rate is then precisely defined, and the conversion predicted above could be checked at a single redshift.

Measuring supernova rate densities is not easy, since supernovae are infrequent in individual galaxies. Core-collapse supernovae (Types II, Ib, Ic) are fainter and

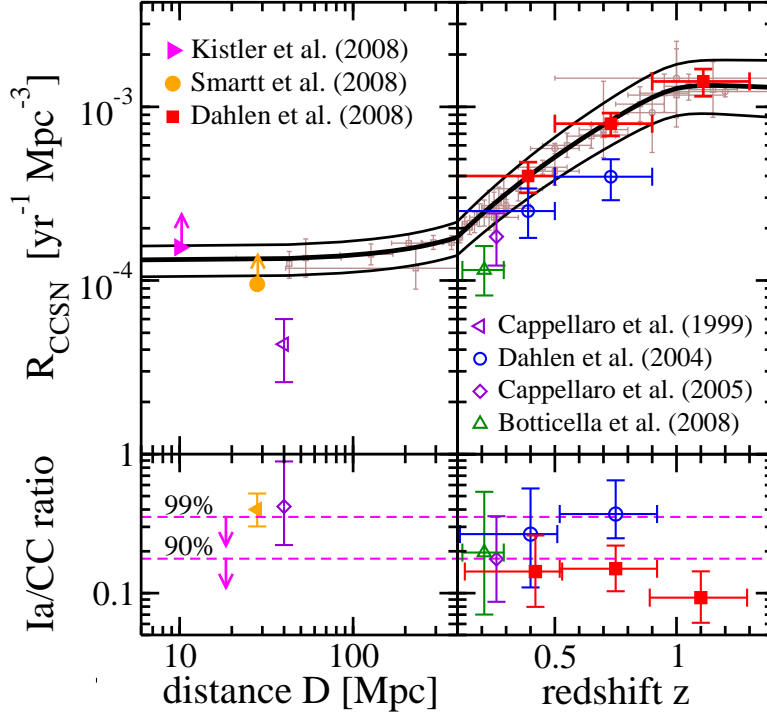


Figure 3: **Predicted and measured cosmic core-collapse supernova rates.** In the upper panel, the band and its width indicate the absolute prediction and its uncertainty from the star formation rate data alone (shown, scaled down, with faint grey points). The most reliable supernova rate measurements are shown with solid symbols; those with open symbols must be less complete. In the lower panel, rate ratios are shown, which supports this. Figure as shown in Ref. (23).

less uniform in their optical properties than the thermonuclear supernovae (Type Ia) used as distance indicators, and have received much less attention, despite being more common.

At high redshift, repeat imaging of a volume can find supernovae largely independent of their host galaxies. This directly measures the quantity of interest. At low redshift, galaxies from a catalog can be monitored. Since this finds the galaxies first, and the supernovae second, it is subject to incompleteness due to faint galaxies, and one must carefully define the global volume and time monitored from those for each galaxy. While these corrections are made, catalog surveys tend to find lower supernova rates and less extreme supernovae than volume surveys. Lastly, supernova rates estimated using supernovae that were not collected in a systematic way should be taken only as lower bounds.

The predicted supernova rate density is shown in **Figure 3**. There is very good agreement with the most reliable data, despite the conversion being predicted absolutely, and not fit. The uncertainty on the star formation rate is taken as 20% on  $R_{SF}(z = 0)$ . The predicted supernova rate and its uncertainty are  $R_{SN}(z = 0) = (1.25 \pm 0.25) \times 10^{-4} \text{ Mpc}^{-3} \text{ year}^{-1}$  (recall Section 3.1). At redshift zero, the lower limits on the rates are already quite high, matching the prediction well; the 10 Mpc was defined very conservatively, and this and the 28 Mpc point are known to be incomplete (52, 87). Therefore, supernova rate

measurements lower than this band *must be less complete*, since the shape is fixed from the star formation rate. At high redshift, the updated Dahlen et al. points are in excellent agreement; these were measured volumetrically (90, 91), and are larger than points that were not (92–94). [After Ref. (23) was published, the Dahlen et al. points decreased slightly, but are still consistent with the band shown in **Figure 3** (T. Dahlen, private communication, 2010).] That faint core-collapse supernovae were missed is supported by data on their rate relative to the brighter Type Ia supernovae. Note that the discovery rates of supernovae have dramatically increased with time, with advances in technology and interest.

The agreement of the predicted and measured supernova rates strongly supports this input for the DSNB calculation. While a significant fraction,  $\sim 50\%$ , of dark collapses is allowed, this is not required ( $\sim 10\%$  is expected). These collapses might be intrinsically faint, truly dark, or just obscured. In any case, their existence can only raise the level of the DSNB. In the near future, supernova rate measurements will greatly improve, and their comparison with star formation rate data will allow more precise tests of the fraction of dark collapses (23, 95–97).

## 6 Third Ingredient: Neutrino Interactions and Detectors

The detection probability depends on the product of the DSNB flux and the effective area of the detector. Since SK (and Earth) is nearly transparent to neutrinos, the effective area is the neutrino-proton cross section times the number of target protons, independent of the shape or orientation of the detector.

While supernovae make all flavors of neutrinos and antineutrinos, the best prospects are for  $\bar{\nu}_e$  in SK, detected by  $\bar{\nu}_e + p \rightarrow e^+ + n$ , as it has both large size and low background rates. The properties of neutrinos are now measured well, and exotic scenarios that would affect DSNB detection, e.g., large mixing with sterile species, are no longer favored.

### 6.1 Detection of DSNB Electron Antineutrinos

Electron antineutrinos are detected by the inverse beta decay reaction on free protons,  $\bar{\nu}_e + p \rightarrow e^+ + n$ . Here “free” protons means hydrogen nuclei, and not the protons bound in heavier nuclei, for which nuclear binding effects suppress interactions at low energies; the atomic ionization state is irrelevant.

The total cross section for inverse beta decay is

$$\sigma(E_\nu) = [0.0952 \times 10^{-42} \text{ cm}^2 (E_\nu - 1.3 \text{ MeV})^2] (1 - 7E_\nu/M_p), \quad (7)$$

for neutrino energies above threshold,  $E_\nu > 1.8 \text{ MeV}$ , and where  $M_p$  is the proton mass (for  $c = 1$ ). In the high-energy range, the rising cross section helps offset the falling flux spectrum. This expression, which is good to the several-percent level in the relevant energy range, neglects the small positron mass but does include the few-tens-percent recoil-order corrections, shown outside the square brackets. At the same orders, the kinematic relationship is

$$E_e = [(E_\nu - 1.3 \text{ MeV})] (1 - E_\nu/M_p), \quad (8)$$

where the isotropy of the neutrino angular distribution has been taken into account. The recoil-order correction to the kinematics can be neglected relative to the detector energy resolution. Full expressions for the cross section and kinematics are given in Ref. (98, 99).

## 6.2 The Super-Kamiokande Detector

The fiducial volume of SK contains 22.5 kton of water, and hence  $1.5 \times 10^{33}$  free protons (100). To reduce backgrounds, SK is under more than 1 km of rock, is heavily shielded by separate outer and inner buffer regions, and was constructed to maintain extreme purity. SK is large enough to have a few DSNB interactions per year, and already has low background rates. These facts are fortuitous, as the SK design was optimized not for the DSNB, but for measurements of proton decay, and atmospheric, accelerator, solar, and Milky Way supernova neutrinos.

In SK, relativistic charged particles are detected by the cones of optical Čerenkov light produced as they lose energy; the Čerenkov process is a small component of the energy loss rate, but is the only one that SK detects directly. The Čerenkov light travels through water to the photomultiplier tubes on the walls, which view a homogeneous volume of transparent water. From the patterns of received photons, the position, direction, energy, and identity of charged particles are determined. SK has excellent detection efficiency for the energies considered here.

## 7 Framework Redux: DSNB Detection Spectrum at Earth

Now that we have reviewed the three ingredients – the supernova neutrino emission, cosmic supernova rate, and detector capabilities – we return to the framework for the DSNB detection spectrum at Earth.

The *event rate spectrum*, in units  $\text{s}^{-1} \text{MeV}^{-1}$ , where the detection cross section  $\sigma(E_\nu)$ , the number of proton targets  $N_p$ , and the shift between neutrino energy  $E_\nu$  and positron energy  $E_e \simeq E_\nu - 1.3 \text{ MeV}$  have been accounted for, is

$$\frac{dN_e}{dE_e}(E_e) = N_p \sigma(E_\nu) \int_0^\infty \left[ (1+z) \varphi[E_\nu(1+z)] \right] \left[ R_{SN}(z) \right] \left[ \left[ \frac{c dt}{dz} \right] dz \right]. \quad (9)$$

For relevant energies, those above 10 MeV, the effective upper limit on the line of sight integral is  $z \sim 1-2$ , as beyond there the falling  $dt/dz$  is no longer compensated by a rising  $R_{SN}(z)$  and the larger emission energies required for the same observed energy probe further into the high-energy tail of the emission spectrum.

In **Figure 4**, we show predictions for the DSNB detection spectrum, taking up-to-date inputs and their uncertainties into account. The range due to different emission parameters, especially at high energies, indicates the uncertainties to be reduced by measuring the DSNB. The uncertainty on the supernova rate is already modest and will soon be smaller. The detection reaction is inverse beta decay in SK, which is well understood. This predicted event rate spectrum can be directly compared with measured data, which are a combination of DSNB signal and detector backgrounds. The DSNB is especially sensitive to the important high-energy part of the emission spectrum. The predictions for different temperatures converge near 10 MeV, so a measurement there would probe  $E_{\bar{\nu}_e, tot}$  alone; the falloff of the spectrum would then probe  $E_{\bar{\nu}_e, avg}$  alone.

## 8 Super-Kamiokande 2003 Upper Limit on the DSNB

It takes extraordinary efforts to operate a gigantic detector like SK with low background rates at low energies. The SK DSNB limit (101) improved upon the Kam-II limit (102) by a factor  $\sim 100$ , establishing the only experimental limit within range of contemporary predictions, an extremely important achievement.

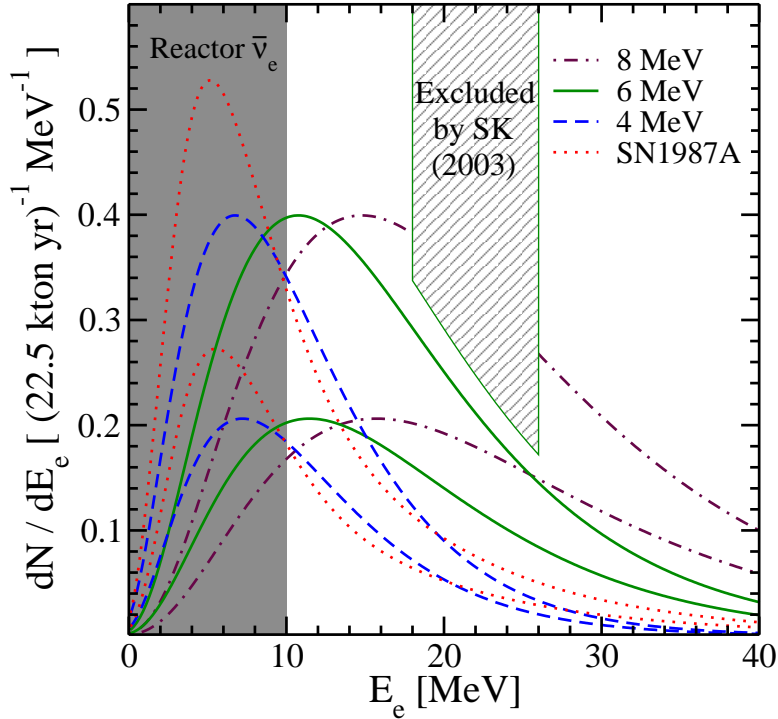


Figure 4: **Predicted DSNB  $\bar{\nu}_e$  event rate spectrum in positron energy.** The labeled bands and their widths are as in **Figure 1**. Integrated event rates are tabulated in Ref. (23). The 2003 exclusion from SK is shown; it is largely independent of the assumed temperature. The energy range of the irreducible reactor background is shaded; backgrounds at higher energies depend on if gadolinium is added to SK. Figure as shown in Ref. (23).

### 8.1 Detector Backgrounds and DSNB Flux Limit

For the SK 2003 DSNB search, only visible positron or electron (they cannot be distinguished) energies above 18 MeV were used, where detector background rates, due to atmospheric neutrinos, are relatively low. Nothing beyond expectations was found in this pioneering search, including any surprise problems that would impede this or improved future searches.

To understand the atmospheric neutrino backgrounds, it is essential to use the event rate spectrum in visible energy. The flux spectrum alone is misleading, as here the visible energy is quite different than the neutrino energy, unlike for the DSNB signal. The backgrounds, shown in **Figure 5** with visible energies of 18–82 MeV, arise from neutrinos with energies up to  $\sim 250$  MeV that invisibly enter the detector and have charged-current interactions, mostly with oxygen nuclei, inside the fiducial volume.

Atmospheric  $\nu_\mu$  and  $\bar{\nu}_\mu$  can produce nonrelativistic  $\mu^-$  and  $\mu^+$ , which do not produce Čerenkov light as they lose energy. When these decay at rest, the electrons and positrons produced are relativistic, and their spectrum is the bump in **Figure 5**. This is the dominant background, but its shape is fixed and its normalization can be measured above the energy range of the DSNB. Atmospheric  $\nu_e$  and  $\bar{\nu}_e$  can produce  $e^-$  and  $e^+$  with energies well below the neutrino energy, due to nuclear effects. These produce the rise at high energies in **Figure 5**.



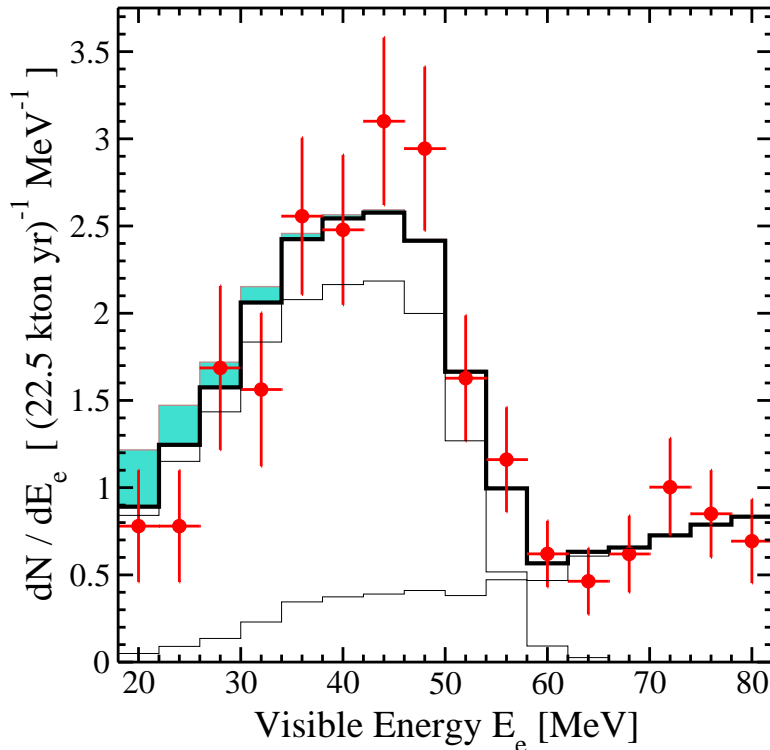


Figure 5: **Results of the SK 2003 DSNB  $\bar{\nu}_e$  search.** The efficiency-corrected measured data are shown with points and error bars. The expected total atmospheric neutrino background is shown by the thick solid line, and its components by the thin solid lines. The largest allowed DSNB signal is shown by the shaded region added to the atmospheric background. Figure adapted from Ref. (101): here  $dN/dE_e$  is shown, to be directly compared in 1-MeV steps to **Figure 4**; to recover the  $dN$  results shown in Ref. (101), multiply the bin values by 4 MeV.

A DSNB signal would have appeared as an excess at low energies (compare to **Figure 4**); none was seen, and a limit of  $\phi(E_\nu > 19.3 \text{ MeV}) \lesssim 1.2 \text{ cm}^{-2} \text{ s}^{-1}$  at the 90% confidence level was set (101).

## 8.2 Calculated Limits on Supernova Neutrino Emission

A DSNB limit expressed as a flux integrated above a certain energy, while a good starting point, is model-dependent and makes comparisons difficult. One variable is not enough to characterize DSNB spectra, but the two natural variables of total energy  $E_{\bar{\nu}_e, \text{tot}}$  and average energy  $E_{\bar{\nu}_e, \text{avg}}$  for the  $\bar{\nu}_e$  flavor are sufficient (47). These directly control our ignorance of the effective supernova neutrino emission, since the cosmic supernova rate is now known well enough. This reinterpretation of the SK DSNB limit, showing how the two emission parameters can compensate each other, is shown in **Figure 6**. Any change in the assumed normalization  $R_{SN}(z=0)$  corresponds to a simple change in  $E_{\bar{\nu}_e, \text{tot}}$  alone, and uncertainties on the evolution  $R_{SN}(z)/R_{SN}(z=0)$  are small.

Excitingly, the sensitivity is near the parameters of supernova models (59–62) and the uncertain fits to the SN 1987A data (103). A two-parameter limit on the effective  $\bar{\nu}_e$  emission is simple for experimentalists to implement and corresponds

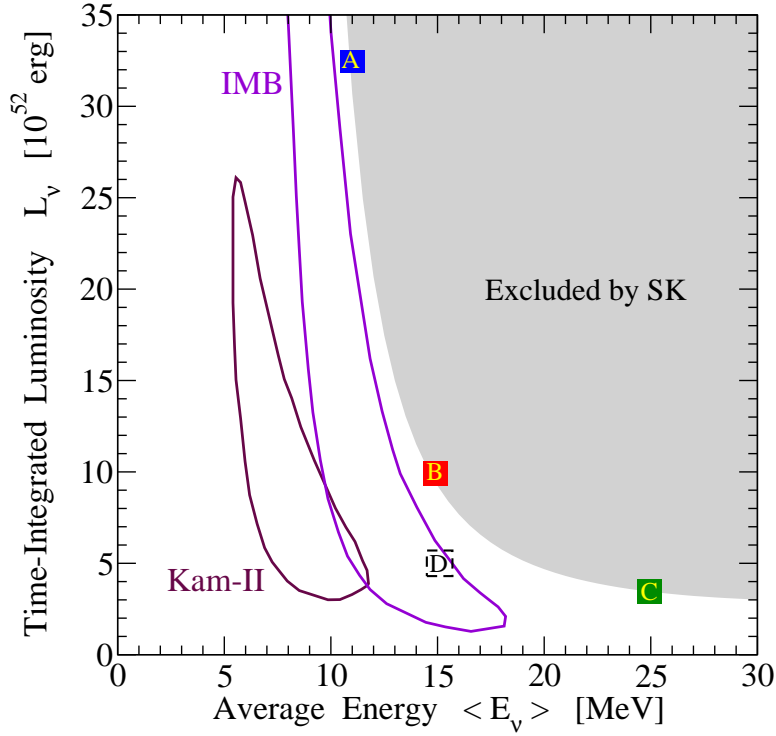


Figure 6: **Constraints on the effective supernova  $\bar{\nu}_e$  emission parameters.** The grey excluded region follows from the null result of the SK 2003 DSNB search. Approximate regions from fits to the SN 1987A data are shown, e.g., Ref. (103). The point D indicates the nominal parameter values. Figure as shown in Ref. (47).

to the minimal theory. If it is proven that there is large variety in supernova neutrino emission, large neutrino mixing effects, or exotic effects, then appropriate theoretical averages should be compared to this direct experimental limit.

## 9 Pathways to Discovery

Progress on experimental sensitivity will have a decisive impact, as the expected signal is close to current limits. Astronomical observations and theoretical work will refine and enhance these prospects.

There are two striking features of the SK 2003 results. First, in the energy range used, the search is background-limited, so the sensitivity will not improve linearly with exposure time, but naively only with the square root. Second, going to lower energies would give much more DSNB signal and much less atmospheric neutrino background; however, there is a large background rate due to the beta decays of nuclei produced by spallation interactions of cosmic-ray muons. To detect the DSNB, SK therefore needs to reduce backgrounds and extend the search to lower energies. But how?

### 9.1 Proposal for Background Reduction in SK

Since the DSNB detection reaction is  $\bar{\nu}_e + p \rightarrow e^+ + n$ , while the detector background reactions mostly do not produce neutrons, it is obvious that neutron

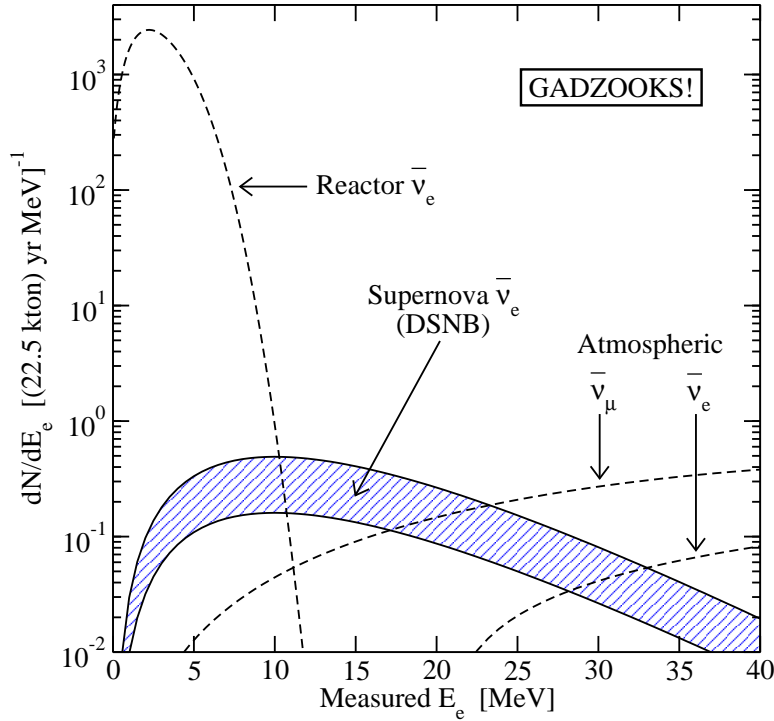


Figure 7: **Expected detection rates in SK with dissolved gadolinium.** The DSNB signal could be cleanly detected at a reasonable rate (see **Figure 4** for updated DSNB predictions and uncertainties). Figure as shown in Ref. (104).

detection is the key to separating signal from backgrounds. The neutron loses energy by elastic scattering and, at present, captures on a free proton, producing a 2.2-MeV gamma ray that leads to an insufficient detection signal in SK.

The idea of positron-neutron coincidence detection goes back to Reines and Cowan, and it is well known how to implement this in oil-and-scintillator detectors, which have much higher light yields than water-Čerenkov detectors. For example, with the suspension of a small concentration of a gadolinium compound in the oil, neutrons will capture on gadolinium, due to its enormous cross section, producing an easily detectable 8-MeV gamma-ray signal. The neutron is detected a long tens of microseconds after the positron, at nearly the same position.

However, until Ref. (104), it had not been shown that neutron detection with dissolved gadolinium in a water-Čerenkov detector could be feasible. The key points are that soluble compounds exist, e.g.,  $\text{GdCl}_3$  and  $\text{Gd}_2(\text{SO}_4)_3$ , and that the gamma rays would lead to a detectable signal in SK, due to its high photomultiplier coverage. That these and many other technical concerns had positive answers was quite surprising. The ability to detect neutrons would give unprecedented capabilities to separate signals and backgrounds in very large detectors. As described in Ref. (104), this would reduce the atmospheric neutrino backgrounds and, more importantly, would dramatically reduce the large spallation radioactivity backgrounds, allowing SK to reduce its DSNB analysis threshold to about 10 MeV, below which the reactor  $\bar{\nu}_e$  background is overwhelming.

**Figure 7** shows that there would be excellent prospects for the DSNB if SK had a  $\sim 0.1\%$  concentration of dissolved gadolinium. There is no known astrophysical

source that can produce a comparable high-energy  $\bar{\nu}_e$  flux, leaving a detection window for the DSNB. If an exotic process converts a small fraction of solar  $\nu_e$  to  $\bar{\nu}_e$ , then the discovery of this new physics could partially get in the way of the DSNB, but we should have such problems (104, 105).

## 9.2 Research and Development for Gadolinium in SK

From the time of Ref. (104), Vagins, aided by other SK experimentalists, has been intensively researching the practicalities of introducing a dissolved gadolinium compound into SK, e.g., Refs. (106–109). Our initial investigations, and the more extensive research that followed, have uncovered no insurmountable problems regarding the infrastructure required to manage the gadolinium, the effects on the detector and other physics searches, or the positron-neutron coincidence detection. However, it has been determined that it is not advisable to pack a kilogram of white  $\text{GdCl}_3$  powder in carry-on luggage for an international flight.

The progress on the comprehensive research and development program, and the seriousness with which the SK Collaboration is considering adding gadolinium, can be illustrated with two recent examples. First, a small container of gadolinium-loaded water and a neutron source were lowered into SK, and it was found that the detectable signal of neutron capture on gadolinium works as expected (110) (see also Ref. (111)). Second, a new 200-ton “miniature” ( $\sim 1\%$  scale) of SK with dissolved gadolinium is being built underground near SK to test all aspects of a gadolinium-loaded water-Čerenkov detector (112).

## 9.3 Prospects for Other Detectors and Flavors

Oil-and-scintillator detectors the size of SK would have reduced atmospheric backgrounds, but the same DSNB signal rate and a reactor background that is relatively large at any location on Earth (113, 114). Ultimately, a high-statistics measurement of DSNB  $\bar{\nu}_e$  will be needed to fully develop the science possibilities, probably with a water-Čerenkov detector at least ten times larger than SK, as is being considered for other purposes (115, 116); the prospects for a high-statistics DSNB measurement have been explored (117–121).

Direct DSNB limits on other neutrino flavors are weaker than for  $\bar{\nu}_e$  in SK. With all their data analyzed, the Sudbury Neutrino Observatory sensitivity to DSNB  $\nu_e$  will only be several times worse (122, 123), comparable to indirect limits (124), but limits for other flavors are worse by orders of magnitude (125, 126). Large liquid-argon detectors are promising for DSNB  $\nu_e$  (127, 128).

## 10 Conclusions

Neutrino astronomy can revolutionize astrophysics and physics, due to its unique abilities to see unseen processes and to probe subtle new particle interactions. Stellar fusion reactions and the core-collapse mechanism were revealed by the detection of neutrinos from the Sun and the nearby SN 1987A. Solar neutrinos were crucial to the discovery of neutrino mixing, and supernova neutrinos probed exotic physics far beyond the reach of laboratory experiments.

However, the great promise of neutrino astronomy remains largely unfulfilled, as no other neutrino sources have yet been detected. Recall the courage of the pioneers of this field, who, more than forty years ago, had neither adequate

detectors nor accurate astrophysics to fortify their hopes. We have advantages of many orders of magnitude on each, and can see the end of the desert. To make progress on our understanding of supernovae and their role in astrophysics, as well as of the neutrinos themselves, we must detect more supernova neutrinos.

Fortunately, first detection of the DSNB is within reach. Why are we so sure?

- **The framework for calculating the DSNB is solid.**

It is built on simple principles of cosmology, well tested with photons.

- **Supernova neutrino emission has been measured from SN 1987A.**

Theory and indirect evidence suggest it should typically be larger.

- **The uncertainty on the cosmic supernova rate is modest.**

Observations of massive stars and supernovae are precise and quickly improving.

- **All aspects of DSNB signal detection are understood.**

Neutrino interactions and detector properties have each been well measured.

Therefore, even including uncertainties, there is a robust prediction that *there must be a few DSNB neutrino events per year in SK*. These events are hidden by backgrounds – what about the experimental prospects for revealing them?

- **SK has already shown sensitivity quite close to these predictions.**

Importantly, SK has controlled detector backgrounds nearly to the required level.

- **There are good prospects for improving the SK DSNB sensitivity.**

With gadolinium, SK would reduce its backgrounds and energy threshold.

Therefore, the DSNB could be discovered in SK. With sufficient detector background reduction, even a few signal events will be statistically significant and scientifically important. If the DSNB is not found, there must be surprising new physics, requiring an upheaval in astrophysics or exotic new particle physics.

The enduring value of a DSNB measurement will come from its comparison to other observations and theory, which include the SN 1987A data and numerical simulations of core collapse. The SK 2003 limit is already an important new result, as it excludes neutrino emission as large as often assumed, and is only a factor 2–4 away from more conservative cases. Significant developments in the theoretical predictions are also eagerly anticipated, as, after more than forty years of work, recent results have increasingly realistic physics and accurate calculations, show explosions in some cases, and some are able to integrate to several seconds. These models will provide a rich context for interpreting DSNB results and, eventually, to novel tests of neutrino properties and other new physics.

In the next several years, we will gain a newly deep and comprehensive understanding of supernovae and their neutrinos, following from the above improvements converging with unprecedented electromagnetic data, results from gravitational wave observatories, and, with a little luck, a Milky Way neutrino burst.

## DISCLOSURE STATEMENT

The author is not aware of any affiliations, memberships, funding, or financial holdings that might be perceived as affecting the objectivity of this review.

## ACKNOWLEDGMENTS

The author's research was supported by NSF CAREER Grant PHY-0547102.

I am grateful to my collaborators on the DSNB – Shin'ichiro Ando, Eli Dwek, Brian Fields, Andrew Hopkins, Shunsaku Horiuchi, Amy Lien, Louie Strigari, Mark Vagins, Terry Walker, Hasan Yüksel, and Pengjie Zhang – as well as to my additional collaborators on closely-related topics – Dick Boyd, Will Farr, Joe Formaggio, Matt Kistler, Chris Kochanek, Tony Mezzacappa, José Prieto, Matthew Sharp, Kris Stanek, Yoichiro Suzuki, Todd Thompson, and Petr Vogel – for sharing their knowledge, enthusiasm, and wisdom.

I especially thank Shin'ichiro Ando, Andrew Hopkins, Shunsaku Horiuchi, Todd Thompson, Mark Vagins, and Hasan Yüksel for helpful comments on the draft manuscript.

## LITERATURE CITED

1. Freedman SJ, et al. arXiv:physics/0411216 (2004)
2. Bethe H, Peierls R. *Nature* 133:532 (1934)
3. Cowan CL, et al. *Science* 124:103 (1956)
4. Reines F, Cowan CL. *Nature* 178:446 (1956)
5. Marx G, Menyhard N. *Science* 131:299 (1960)
6. Pontecorvo B. *Sov. Phys. Usp.* 6:1 (1963)
7. Bahcall JN. *Science* 147:115 (1965)
8. Ruderman MA. *Rept. Prog. Phys.* 28:411 (1965)
9. Bahcall JN. *Phys. Rev. Lett.* 12:300 (1964)
10. Bahcall JN. *Neutrino Astrophysics*. Cambridge, UK: Cambridge Univ. Press. 584 pp. (1989)
11. Learned JG, Mannheim K. *Ann. Rev. Nucl. Part. Sci.* 50:679 (2000)
12. Anchordoqui LA, Montaruli T. arXiv:0912.1035 (2009)
13. Beatty JJ, Westerhoff S. *Ann. Rev. Nucl. Part. Sci.* 59:319 (2009)
14. Arnett WD, Bahcall JN, Kirshner RP, Woosley SE. *Ann. Rev. Astron. Astrophys.* 27:629 (1989)
15. Hirata K, et al. *Phys. Rev. Lett.* 58:1490 (1987)
16. Hirata KS, et al. *Phys. Rev. D* 38:448 (1988)
17. Bionta RM, et al. *Phys. Rev. Lett.* 58:1494 (1987)
18. Bratton CB, et al. *Phys. Rev. D* 37:3361 (1988)
19. Ando S. *Phys. Lett. B* 570:11 (2003)
20. Fogli GL, Lisi E, Mirizzi A, Montanino D. *Phys. Rev. D* 70:013001 (2004)
21. Goldberg H, Perez G, Sarcevic I. *JHEP* 11:023 (2006)
22. Baker J, Goldberg H, Perez G, Sarcevic I. *Phys. Rev. D* 76:063004 (2007)
23. Horiuchi S, Beacom JF, Dwek E. *Phys. Rev. D* 79:083013 (2009)
24. Nakazato K, Sumiyoshi K, Suzuki H, Yamada S. *Phys. Rev. D* 78:083014 (2008)
25. Zel'dovich YB, Guseinov OK. *Sov. Phys. Dok.* 10:524 (1965)
26. Guseinov OK. *Sov. Astron.* 10:613 (1967)
27. Bisnovatyi-Kogan GS, Seidov ZF. *Sov. Astron.* 26:132 (1982)
28. Domogatskii GV. *Sov. Astron.* 28:30 (1984)

29. Krauss LM, Glashow SL, Schramm DN. *Nature* 310:191 (1984)
30. Bisnovatyi-Kogan GS, Seidov ZF. *Ann. New York Acad. Sci.* 422:319 (1984)
31. Lagage PO. *Nature* 316:420 (1985)
32. Dar A. *Phys. Rev. Lett.* 55:1422 (1985)
33. Woosley SE, Wilson JR, Mayle R. *Astrophys. J.* 302:19 (1986)
34. Schramm DN, Mayle R, Wilson JR. *Nuovo Cim. C* 9:443 (1986)
35. Totani T, Sato K, Yoshii Y. *Astrophys. J.* 460:303 (1996)
36. Malaney RA. *Astropart. Phys.* 7:125 (1997)
37. Hartmann DH, Woosley SE. *Astropart. Phys.* 7:137 (1997)
38. Kaplinghat M, Steigman G, Walker TP. *Phys. Rev. D* 62:043001 (2000)
39. Ando S, Sato K, Totani T. *Astropart. Phys.* 18:307 (2003)
40. Fukugita M, Kawasaki M. *Mon. Not. Roy. Astron. Soc.* 340:L7 (2003)
41. Strigari LE, Kaplinghat M, Steigman G, Walker TP. *JCAP* 0403:007 (2004)
42. Iocco F, et al. *Astropart. Phys.* 23:303 (2005)
43. Strigari LE, Beacom JF, Walker TP, Zhang P. *JCAP* 0504:017 (2005)
44. Daigne F, Olive KA, Sandick P, Vangioni E. *Phys. Rev. D* 72:103007 (2005)
45. Lunardini C. *Astropart. Phys.* 26:190 (2006)
46. Ando S, Sato K. *New J. Phys.* 6:170 (2004)
47. Yüksel H, Ando S, Beacom JF. *Phys. Rev. C* 74:015803 (2006)
48. Hansen CJ, Kawaler SD. *Stellar Interiors. Physical Principles, Structure, and Evolution.* Berlin: Springer Verlag. 445 pp. (1994)
49. Kennicutt RC. *Astrophys. J.* 277:361 (1984)
50. Heger A, et al. *Astrophys. J.* 591:288 (2003)
51. Filippenko AV. *Ann. Rev. Astron. Astrophys.* 35:309 (1997)
52. Kistler MD, et al. arXiv:0810.1959 (2008)
53. Raffelt GG. *Stars as Laboratories for Fundamental Physics.* Chicago : Univ. Chicago Press. 664 pp. (1996)
54. Horowitz CJ, Piekarewicz J. *Phys. Rev. Lett.* 86:5647 (2001)
55. Page D, Reddy S. *Ann. Rev. Nucl. Part. Sci.* 56:327 (2006)
56. Lattimer JM, Prakash M. *Phys. Rept.* 442:109 (2007)
57. Zhang W, Woosley SE, Heger A. *Astrophys. J.* 679:639 (2008)
58. Fryer CL. *Astrophys. J.* 699:409 (2009)
59. Mezzacappa A. *Ann. Rev. Nucl. Part. Sci.* 55:467 (2005)
60. Ott CD, Burrows A, Dessart L, Livne E. *Astrophys. J.* 685:1069 (2008)
61. Janka HT, et al. *Phys. Rept.* 442:38 (2007)
62. Huedepohl L, et al. arXiv:0912.0260 (2009)
63. Yüksel H, Beacom JF. *Phys. Rev. D* 76:083007 (2007)
64. Keil MT, Raffelt GG, Janka HT. *Astrophys. J.* 590:971 (2003)
65. Dighe AS, Smirnov AY. *Phys. Rev. D* 62:033007 (2000)
66. Fetter J, McLaughlin GC, Balantekin AB, Fuller GM. *Astropart. Phys.* 18:433 (2003)
67. Duan H, Fuller GM, Carlson J, Qian YZ. *Phys. Rev. Lett.* 97:241101 (2006)
68. Dasgupta B, Dighe A, Raffelt GG, Smirnov AY. *Phys. Rev. Lett.* 103:051105 (2009)
69. Ando S, Sato K. *Phys. Lett. B* 559:113 (2003)
70. Woosley SE, Haxton WC. *Nature* 334:45 (1988)
71. Heger A, et al. *Phys. Lett. B* 606:258 (2005)
72. Yoshida T, Kajino T, Hartmann DH. *Phys. Rev. Lett.* 94:231101 (2005)
73. Salpeter EE. *Astrophys. J.* 121:161 (1955)
74. Baldry IK, Glazebrook K. *Astrophys. J.* 593:258 (2003)

75. Kennicutt RC. *Ann. Rev. Astron. Astrophys.* 36:189 (1998)
76. Hopkins AM, Beacom JF. *Astrophys. J.* 651:142 (2006)
77. Yüksel H, Kistler MD, Beacom JF, Hopkins AM. *Astrophys. J.* 683:L5 (2008)
78. Kistler MD, et al. *Astrophys. J.* 705:L104 (2009)
79. Butler NR, Bloom JS, Poznanski D. arXiv:0910.3341 (2009)
80. Oesch PA, et al. arXiv:0909.1806 (2009)
81. Bouwens RJ, et al. *Astrophys. J.* 705:936 (2009)
82. Yan H, et al. arXiv:0910.0077 (2009)
83. Gal-Yam A, et al. *Astrophys. J.* 656:372 (2007)
84. Li WD, et al. *Astrophys. J.* 661:1013 (2007)
85. Prieto JL, et al. *Astrophys. J.* 681:L9 (2008)
86. Smartt SJ. *Ann. Rev. Astron. Astrophys.* 47:63 (2009)
87. Smartt SJ, Eldridge JJ, Crockett RM, Maund JR. *Mon. Not. Roy. Astron. Soc.* 395:1409 (2009)
88. Kalirai JS, et al. *Astrophys. J.* 676:594 (2008)
89. Williams KA, Bolte M, Koester D. *Astrophys. J.* 693:355 (2009)
90. Dahlen T, et al. *Astrophys. J.* 613:189 (2004)
91. Dahlen T, et al. Arcetri Supernova Rates Workshop (2008)  
<http://www.arcetri.astro.it/filippo/snrate08/Home.html>
92. Cappellaro E, Evans R, Turatto M. *Astron. Astrophys.* 351:459 (1999)
93. Cappellaro E, et al. *Astron. Astrophys.* 430:83 (2005)
94. Botticella MT, et al. *Astron. Astrophys.* 479:49 (2008)
95. Kochanek CS, et al. *Astrophys. J.* 684:1336 (2008)
96. Lunardini C. *Phys. Rev. Lett.* 102:231101 (2009)
97. Lien A, Fields BD, Beacom JF. *Phys. Rev. D* 81:083001 (2010)
98. Vogel P, Beacom JF. *Phys. Rev. D* 60:053003 (1999)
99. Strumia A, Vissani F. *Phys. Lett. B* 564:42 (2003)
100. Fukuda Y, et al. *Nucl. Instrum. Meth. A* 501:418 (2003)
101. Malek M, et al. *Phys. Rev. Lett.* 90:061101 (2003)
102. Zhang W, et al. *Phys. Rev. Lett.* 61:385 (1988)
103. Jegerlehner B, Neubig F, Raffelt G. *Phys. Rev. D* 54:1194 (1996)
104. Beacom JF, Vagins MR. *Phys. Rev. Lett.* 93:171101 (2004)
105. Raffelt G, Rashba T. arXiv:0902.4832 (2009)
106. Vagins MR, Svoboda RC. Funded proposal to the US Dept. of Energy Advanced Detector Research Program (2003)  
[http://www.er.doe.gov/hep/hep\\_ADR/2003ADRWinners.shtml](http://www.er.doe.gov/hep/hep_ADR/2003ADRWinners.shtml)
107. Vagins MR. Funded proposal to the US Dept. of Energy Advanced Detector Research Program (2005)  
[http://www.er.doe.gov/hep/hep\\_ADR/2005ADRWinners.shtml](http://www.er.doe.gov/hep/hep_ADR/2005ADRWinners.shtml)
108. Vagins MR. Funded proposal to the US Dept. of Energy Advanced Detector Research Program (2007)  
[http://www.er.doe.gov/hep/hep\\_ADR/2007ADRWinners.shtml](http://www.er.doe.gov/hep/hep_ADR/2007ADRWinners.shtml)
109. Nakahata M. *J. Phys. Conf. Ser.* 136:022042 (2008)
110. Watanabe H, et al. *Astropart. Phys.* 31:320 (2009)
111. Dazeley S, Bernstein A, Bowden NS, Svoboda R. *Nucl. Instrum. Meth. A* 607:616 (2009)
112. Kibayashi A, et al. arXiv:0909.5528 (2009)
113. Learned JG, Dye ST, Pakvasa S. arXiv:0810.4975 (2008)
114. Würm M, et al. *Phys. Rev. D* 75:023007 (2007)



115. Bernstein A, et al. arXiv:0907.4183 (2009)
116. Autiero D, et al. *JCAP* 0711:011 (2007)
117. Ando S. *Astrophys. J.* 607:20 (2004)
118. Lunardini C. *Phys. Rev. D* 75:073022 (2007)
119. Volpe C, Welzel J. arXiv:0711.3237 (2007)
120. Chakraborty S, Choubey S, Dasgupta B, Kar K. *JCAP* 0809:013 (2008)
121. Galais S, Kneller J, Volpe C, Gava J. arXiv:0906.5294 (2009)
122. Beacom JF, Strigari LE. *Phys. Rev. C* 73:035807 (2006)
123. Aharmim B, et al. *Astrophys. J.* 653:1545 (2006)
124. Lunardini C. *Phys. Rev. D* 73:083009 (2006)
125. Aglietta M, et al. *Astropart. Phys.* 1:1 (1992)
126. Lunardini C, Peres OLG. *JCAP* 0808:033 (2008)
127. Cocco AG, et al. *JCAP* 0412:002 (2004)
128. Rubbia A. *J. Phys. Conf. Ser.* 171:012020 (2009)